DGKE Variants Cause a Glomerular Microangiopathy That Mimics Membranoproliferative GN

Fatih Ozaltin,*† Binghua Li,‡ Alysha Rauhauser,‡ Sung-Wan An,‡ Oguz Soylemezoglu,§ Ipek Isik Gonul,‖ Ekim Z. Taskiran,†¶ Tulin Ibsirlioglu,† Emine Korkmaz,† Yelda Bilginer,* Ali Duzova,* Seza Ozen,* Rezan Topaloglu,* Nesrin Besbas,* Shazia Ashraf,**†† Yong Du,‡‡ Chaoying Liang,‡‡ Phylip Chen,§§ Dongmei Lu,‡ Komal Vadnagara,‡ Susan Arbuckle,‖‖ Deborah Lewis,¶¶ Benjamin Wakeland,‡‡ Richard J. Quigg,*** Richard F. Ransom,††† Edward K. Wakeland,‡‡ Matthew K. Topham,‡‡‡ Nicolas G. Bazan,§§§ Chandra Mohan,‡‡ Friedhelm Hildebrandt,**†† Aysin Bakkaloglu,* Chou-Long Huang,‡ and Massimo Attanasio‡‖‖‖

Departments of *Pediatric Nephrology and Rheumatology and ¶Medical Genetics, Hacettepe University Faculty of Medicine, Ankara, Turkey; †Nephrogenetics Laboratory, Department of Pediatric Nephrology, Hacettepe University Faculty of Medicine, Ankara, Turkey; Departments of ‡Internal Medicine and ‡‡Immunology, University of Texas Southwestern Medical Center, Dallas, Texas; Departments of §Pediatric Nephrology and ‖Pathology, Gazi University Faculty of Medicine, Ankara, Turkey; **Howard Hughes Medical Institute, Chevy Chase, Maryland; ††Department of Pediatrics, University of Michigan, Ann Arbor, Michigan; §§College of Medicine, The Ohio State University, Columbus, Ohio; Departments of ‖‖Histopathology and ¶¶Pediatric Nephrology, The Sydney Children's Hospitals Network, Westmead, Sydney, Australia; ***Department of Medicine, The University of Chicago, Chicago, Illinois; †††The Research Institute at Nationwide Children's Hospital, Columbus, Ohio; ‡‡‡Huntsman Cancer Institute, University of Utah, Salt Lake City, Utah; §§§Louisiana State University, New Orleans, Louisiana; and ‖‖‖Eugene McDermott Center for Growth and Development, University of Texas Southwestern Medical Center, Dallas, Texas

ABSTRACT

Renal microangiopathies and membranoproliferative GN (MPGN) can manifest similar clinical presentations and histology, suggesting the possibility of a common underlying mechanism in some cases. Here, we performed homozygosity mapping and whole exome sequencing in a Turkish consanguineous family and identified *DGKE* gene variants as the cause of a membranoproliferative-like glomerular microangiopathy. Furthermore, we identified two additional *DGKE* variants in a cohort of 142 unrelated patients diagnosed with membranoproliferative GN. This gene encodes the diacylglycerol kinase DGKε, which is an intracellular lipid kinase that phosphorylates diacylglycerol to phosphatidic acid. Immunofluorescence confocal microscopy demonstrated that mouse and rat Dgkε colocalizes with the podocyte marker WT1 but not with the endothelial marker CD31. Patch-clamp experiments in human embryonic kidney (HEK293) cells showed that DGKε variants affect the intracellular concentration of diacylglycerol. Taken together, these results not only identify a genetic cause of a glomerular microangiopathy but also suggest that the phosphatidylinositol cycle, which requires *DGKE*, is critical to the normal function of podocytes.

J Am Soc Nephrol 24: 377–384, 2013. doi: 10.1681/ASN.2012090903

The term *membranoproliferative glomerulonephritis* (MPGN) defines a heterogeneous group of kidney diseases that frequently lead to kidney failure.[1] The distinction of MPGN in three subtypes, based on different pathologic pictures, was recently replaced by a classification that accounts for the pathogenetic mechanisms underlying the diverse observed glomerular lesions. According to the new classification, MPGN is considered to fall in two etiological categories, in which either deposition of Ig or uncontrolled Ig-independent complement activation induces glomerular proliferative/exudative processes that result in mesangial expansion, hyperlobulated glomeruli, and, in the reparative phase,

Received September 11, 2012. Accepted November 27, 2012.

F.O., B.L., and A.R. contributed equally to this work.

Published online ahead of print. Publication date available at www.jasn.org.

Correspondence: Dr. Massimo Attanasio, University of Texas Southwestern Medical Center, 5323 Harry Hines Boulevard, Dallas TX, 75390, or Dr. Fatih Ozaltin, Departments of Pediatric Nephrology and Rheumatology, Hacettepe University Faculty of Medicine, 06100, Sihiye, Ankara, Turkey. Email: massimo.attanasio@utsouthwestern.edu or fozaltin@hacettepe.edu.tr

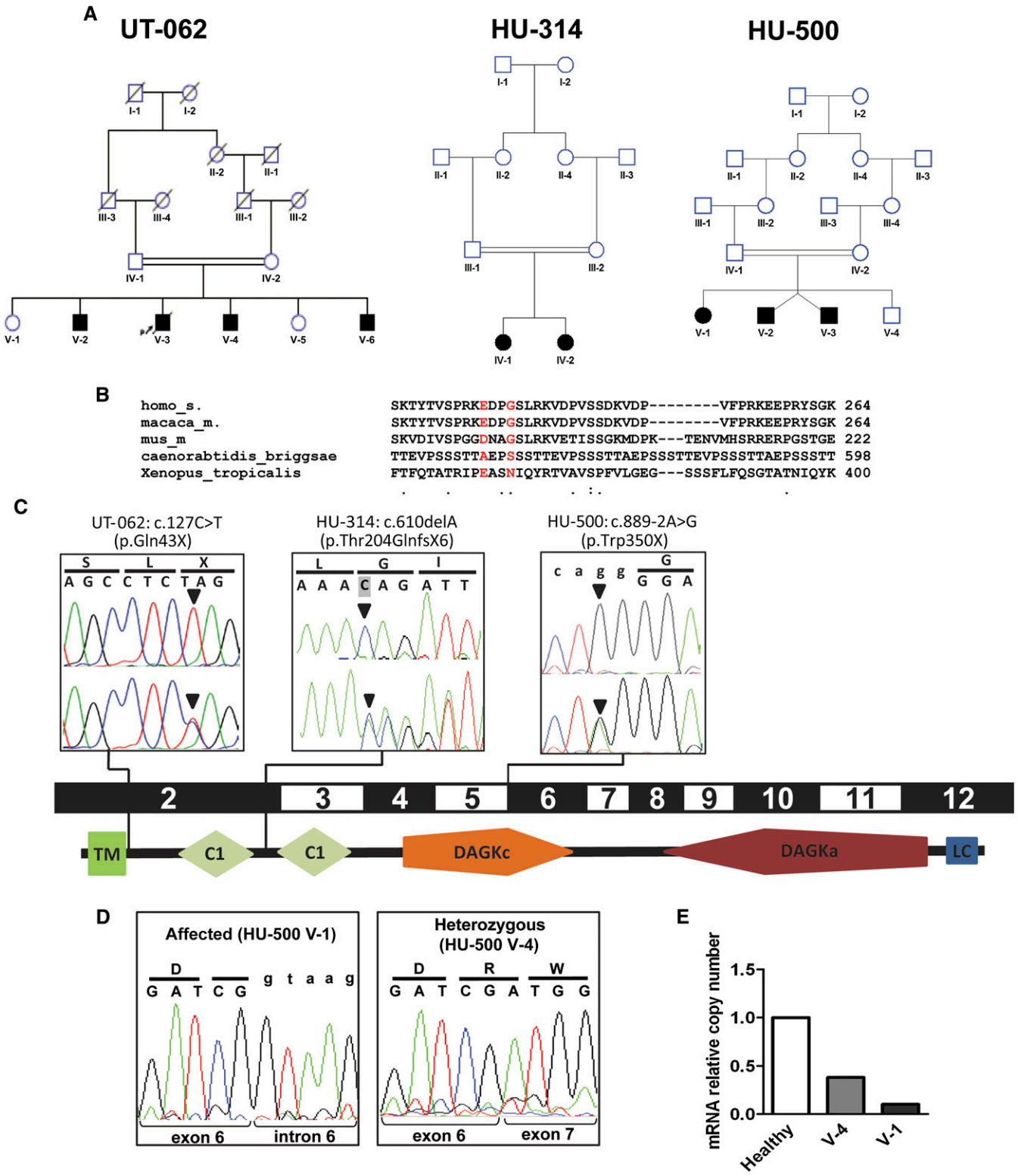

Figure 1. Representation of the pedigrees described in this study and of the *DGKE* mutations in relation to the gene exon structure and protein domains. (A) Pedigrees of families UT-062, HU-314, and HU-500. Squares represent males, circles represent females. Black filled symbols indicate the affected status. Double-horizontal bars indicate consanguinity. (B) Sequence alignment across different species of the GPRIN1 gene in correspondence of the two sequence variants detected by exome sequencing in the affected individuals of family UT-062. The reference amino acids are represented in red. Dots on the bottom line represent medium (:) and low (.) evolutionary conservation. The absence of a dot indicates absence of evolutionary conservation. Numbers indicate the position of the last represented amino acid in

splitting (double contour or "tram track" appearance) of the glomerular basement membrane, thereby causing injury of podocytes, glomerular capillaries, and mesangial cells.[2] Familial occurrence has been described for both primary/idiopathic forms of MPGN[3–6] and for rare forms of thrombotic microangiopathy,[7–10] but little is known about the underlying genetic etiology. We performed homozygosity mapping and whole exome sequencing in a large index family from Turkey with four siblings affected with autosomal recessive disease with histologic signs of MPGN accompanied by prominent endothelial distress to identify genetic variants causative of this admixed phenotype. Participants with clinical and histological diagnosis of MPGN were ascertained and enrolled in the study after obtaining informed consent, in accordance with human participant research protocols approved by the Hacettepe University in Ankara (TBK08/1-57) and by the University of Texas Southwestern Medical Center in Dallas (112006-011).

The two healthy parents as well as two unaffected and three of the four affected individuals of UT-062 (Figure 1 A and C, Figure 2, and Table 1; see the Supplemental Material for a detailed description of the clinical history) were genotyped using the 250K Affymetrix single nucleotide polymorphism array. We identified three uninterrupted homozygous haplotypes that overlapped in all three affected individuals but not in the healthy siblings (Supplemental Figure 1A). Copy number variation analysis (Supplemental Figure 1B) excluded the presence of homozygous deletions within the identified homozygous regions in the affected siblings. The overall length of these regions was 12.3 Mb and included 1206 exons from 253 genes (Supplemental Table 1). Given the high number of exons in the regions, we performed whole exome capture followed by massive parallel sequencing on the DNA of two of the affected siblings (UT-062 V-2 and UT-062 V-4) to discover putative deleterious genetic variants (coverage data are reported in Supplemental Table 2). We identified a total of 30 coding single nucleotide variations within the three shared homozygous intervals, three of which were not annotated in the dbSNP database (build 131). Two of these variants were predicted to result in nonsynonymous changes in two residues of the gene G protein–regulated inducer of neurite outgrowth (GPRIN1) (p.Glu233Val and p.Gly236Val) that are poorly conserved in the evolution (Figure 1B and Supplemental Figure 2). Most importantly, this gene is exclusively expressed in neurons and no transcripts have been detected in the kidney,[11] excluding a causative role for the disease in this family. Furthermore, six loss-of-function variants (two frame shift and four missense mutations predicted to be deleterious by SIFT [sorting tolerant from intolerant] analysis[12]) have been found in GPRIN1 in 628 individuals sequenced in the 1000 Genomes Project[13] and in the 6503 samples of the National Heart, Lung, and Blood Institute Exome Sequencing (NES) Project,[14] indicating that this gene is weakly subject to evolutionary pressure. The third identified single nucleotide variation was a transition from C to T (c.127C>T) in the first coding exon of *DGKE* (NM_003647.2), a gene that encodes the ε isoform of diacylglycerol kinase,[15] and creates a stop codon at glutamine 43 (p.Gln43X) that results in a predicted peptide missing all the functional domains (Figure 1C). The mutation was confirmed by Sanger sequencing and segregated in the pedigree with an autosomal recessive pattern. Because we performed homozygosity mapping,[16] only missense variants within the homozygous identical by descent regions were tested for segregation. To support the causative role of *DGKE* mutations, we used exon sequencing to screen a worldwide cohort of 142 unrelated individuals diagnosed with MPGN. We found a homozygous deletion, c.610delA (p.Thr204GlnfsX6), in two affected siblings from an unrelated consanguineous Turkish family (HU-314) (Figure 1, A and C and Figure 2). The mutation causes a shift in the mRNA reading frame and is predicted to result in the creation of a stop codon at position 210 of the aberrant transcript. We reproduced the two mutations by site-directed mutagenesis in *DGKE* cDNAs cloned in myc-tagging expression vectors. After overexpression in HEK293T cells, our Western blot analysis detected a truncated protein of the predicted size obtained from the mutant c.610delA but not from the c.127C>T mutant (Figure 3A), suggesting that the truncated

the corresponding protein. (C) Chromatograms of the three different mutations in the gene *DGKE* (arrowheads) in the representative affected individuals from the consanguineous pedigrees UT-062, HU-314, and HU-500, in relation to the corresponding coding exons and schematic representation of human DGKε protein structure (according to SMART, http://smart.embl-heidelberg.de). Pedigree identifiers and mutations are reported above the boxes. Upper chromatograms report the homozygous mutations in one affected sibling per each pedigree. Lower chromatograms show the heterozygous mutations in one of the parents from each family. Codons and the corresponding translated amino acids are displayed above the chromatograms. Lowercase letters indicate the intronic sequence. Shading of the first base of the second codon in HU-314 chromatogram indicates the deleted base. (D) Chromatograms of the RT-PCR on mRNA obtained from peripheral leukocytes of one affected individual (V-1) and a heterozygous sibling (V-4) of family HU-500. Intron 6 is retained in the presence of homozygous mutation (left panel), resulting in the transcription of the intron (lowercase letters). Note that in the heterozygous sibling (right panel), only the wild-type allele is detectable, indicating that the amount of mutated mRNA is very low compared with the wild type. Codons and the corresponding translated amino acids are displayed above the chromatograms. Lowercase letters indicate the intronic sequence. (E) Relative quantitation by real-time PCR of the number of *DGKE* transcripts in leukocytes from an healthy individual, an heterozygous carrier, and the homozygous affected individual HU-500 V-1 showing that the mutated transcript undergoes non-sense–mediated decay. TM, transmembrane domain; C1, protein kinase C conserved region (C1 domain); DAGKc, diacylglycerol kinase catalytic domain; DAGKa, diacylglycerol kinase accessory domain; LC, low complexity region.

Table 1. Clinical features of the patients with *DGKE* mutations

Family and Individual	Consanguinity	Nucleotide Alteration[a]	Segregation	Age at Onset (yr)	Proteinuria at Onset[b]	Serum Albumin at Onset ($g \cdot dl^{-1}$)	Serum Creatinine at Onset ($mg \cdot dl^{-1}$)	Age at ESRF (yr) and Outcome	Histology	Last Proteinuria[b]	Last Serum Albumin ($g \cdot dl^{-1}$)	Last Serum Creatinine ($mg \cdot dl^{-1}$)
UT-032												
V-2	Y	c.127C>T(p.Gln43X)	H, M, P	5	4+	2.5	3	8 (transplanted at 20 yr)	MPGN	2+	4	1.46
V-3	Y	c.127C>T(p.Gln43X)	H, M, P	2	4+	2.2	0.6	Died at 4 yr	MPGN	N/A	N/A	N/A
V-4	Y	c.127C>T(p.Gln43X)	H, M, P	4	4+	2.5	0.6	None at 30 yr	MPGN	4+	4	2
V-6	Y	c.127C>T(p.Gln43X)	H, M, P	0.8	4+	2.4	0.6	19	MPGN	4+	4	9.8
HU-314												
IV-1	Y	c.delA 604-610 (p.Thr204GlnfsX6)	H, M, P	17	4+	2.5	1.9	23	MPGN[c]	3+	3.2	4
IV-2	Y	c.delA 604-610 (p.Thr204GlnfsX6)	H, M, P	8	2+	4.8	0.68	None at 19 yr	MPGN	Trace	4	0.9
HU-500												
V-1	Y	c.889-2A>G (p.Trp350X)	H, M, P	1.5	4+	2.8	0.4	None at 12 yr	MPGN	1+	3.9	0.3
V-2	Y	c.889-2A>G (p.Trp350X)	H, M, P	1.5	4+	1.7	0.77	None at 2 yr	MPGN	3+	3.4	0.4
V-3	Y	c.889-2A>G (p.Trp350X)	H, M, P	1.5	4+	2.4	0.34	None at 2 yr	MPGN	4+	2.8	0.3

ESRF, end stage renal failure; H, homozygous in affected individual; M, heterozygous mutation identified in the mother; P, heterozygous mutation identified in the father; N/A, not available.
[a]Nucleotide positions are numbered according to *DGKE* (NM_003647.2). All mutations were absent in 166 healthy Turkish children.
[b]Assessed by urine dipstick.
[c]There were also secondary focal and segmental sclerotic glomeruli, which could be seen in the advanced stage of any glomerulopathy

peptide is rapidly degraded. A third mutation (c.889-2A>G) that abolishes the obligatory acceptor splice site of intron 5 was found in the affected siblings of a family (HU-500) of Lebanese origin from Australia (Figure 1, A and C and Figure 2). We sequenced the *DGKE* cDNA of one of the affected siblings (V-1) and of the carrier healthy siblings (V-4) and found that intron 6 was retained in the presence of the homozygous change but not in the wild type (Figure 1D, Supplemental Figure 3), confirming that the mutation results in an abnormal transcript predicted to create a premature stop codon (amino acid 350, p. Trp350X). Interestingly, we could not amplify the mutated allele from the heterozygote carrier (Figure 1D), which suggested that the number of mutated transcripts is negligible due to nonsense–mediated decay. This hypothesis was confirmed by quantitative real-time PCR (Figure 1E). The mutations c.127C>T and c.889-2A>G were not detected in 332 chromosomes from 166 healthy participants from the same ethnicity, in the 628 individuals of the 1000 Genomes Project[13] and in the 6503 samples of the NES Project.[14] A heterozygous c.610delA change has recently been reported in one individual in the 1000 Genomes Project (added as rs147972030 to dbSNP134) but is not present in the NES cohort. Based on these two databases and on our controls, the minor allele frequency of this change is of 0.0002 (2 of 7297), indicating that this is an extremely rare variant, as is expected for mutations causing rare recessive diseases.[17]

Diacylglycerol kinases (DGKs) are intracellular lipid kinases that are devoted to phosphorylate diacylglycerol (DAG) to phosphatidic acid[18] (Supplemental Figure 4). We determined by immunofluorescence confocal microscopy that Dgkε is expressed in adult mouse and rat kidneys and colocalizes with the podocyte marker WT1[19] but not with the endothelial marker CD31 (Supplemental Figure 5A). Saturation of the antibody with molar excess of an unrelated Dgkε peptide proved the specificity of the immune reaction (Supplemental

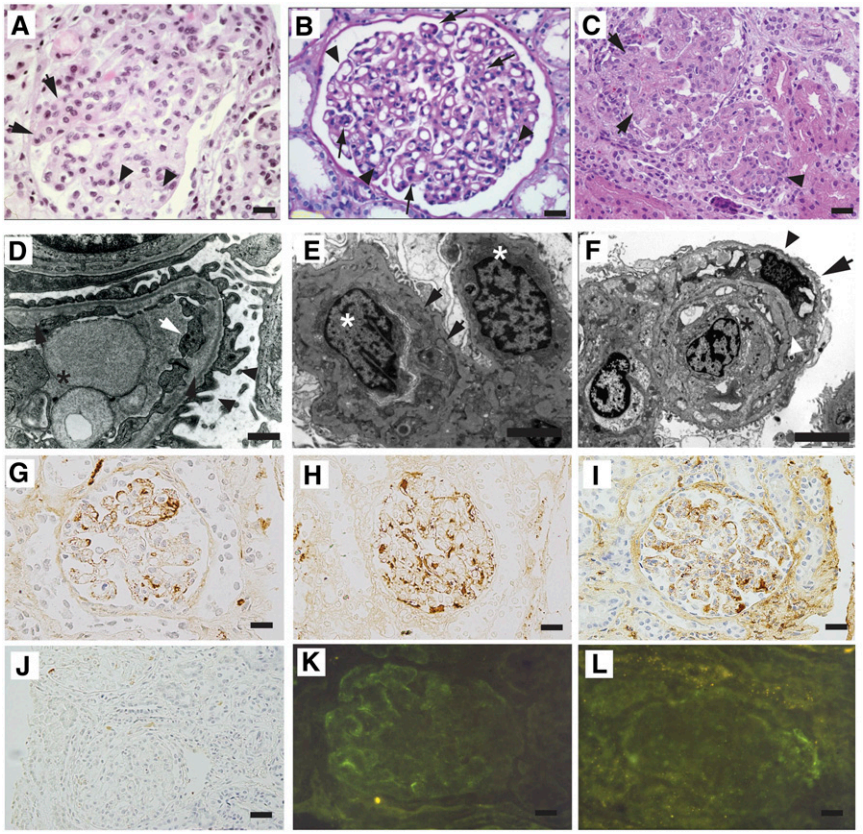

Figure 2. Loss-of-function mutations in DGKE cause MPGN-like glomerular microangiopathy. (A) Kidney biopsy of patient UT-062 V-6. The represented glomerulus is hypertrophic and hypercellular. Focal capillary obliteration and thickening of the basement membrane can also be noticed (arrows) compared with patent capillaries (arrowheads). Hematoxylin and eosin. (B) Periodic acid–Schiff staining of a specimen from patient HU-314 IV-2 shows focal duplication of the glomerular basement membrane (arrowheads), causing thickening of the basement membranes in a hypertrophic glomerulus. (C) Image of the kidney biopsy from patient HU-500 V-1. The represented glomeruli are hypertrophic, hyperlobulated, and hypercellular (arrowhead) and present obliteration of the vascular spaces with endothelial cell swelling (arrows). Hematoxylin and eosin. (D) Transmission electron microscopy image of a glomerulus of patient UT-062 V-6. The capillary lumen is obliterated by the body of an endothelial cell (asterisk). Endothelial cytoplasmic rim is swollen (white arrow). Lamina rara interna is irregularly widened with flocculent material (black arrows). Foot processes on the epithelial side are partially effaced (arrowheads). (E) Electron micrograph of kidney biopsy of patient HU-500 V-1. Two swollen endothelial cells (asterisks) occlude a capillary lumen. The basement membrane is split (arrows) by the interposition of a mesangial cell. Uranyl acetate and lead citrate. (F) Electron micrograph of the kidney biopsy of patient HU-500 V-2. A swollen endothelial cell (asterisk) obstructs the lumen of a capillary. The basement membrane is split (white arrowhead) by the interposition of a mesangial cell (arrow). The podocyte foot processes are effaced (black arrowhead). Uranyl acetate and lead citrate. (G–J) Immunoperoxidase staining of biopsies from patient HU-500 V-1. Segmental deposition of IgM (G) and patchy deposition of IgG (H) are visible. Less intense stain was obtained with anti-C1q (I) and no C3 deposition was detected (J). (K and L) Immunofluorescence microscopy of biopsy from patient UT-062 V-6 showing week peripheral segmental deposition of IgM (K) and no intraglomerular deposits of C3 (L). Scale bar, 20 μm in A–C; 1 μm in E and F; 20 μm in G–L.

Figure 5B). We also detected DGKε by Western blot in human immortalized podocytes and rat kidneys and testes (Supplemental Figure 5, C and D), where the enzyme was previously reported to be expressed.[18] DGKε is the smallest of the known mammalian DGKs and lacks extra-enzymatic regulatory domains,[20] a characteristic that suggests that this isoform is constitutively active. Another distinctive feature of DGKε is its marked substrate selectivity for DAG that is acylated with arachidonic acid at the sn-2 position (sn-2-arachidonoil-DAG). The selectivity for arachidonoil-DAG results in the enrichment with arachidonic acid of the phospholipids that participate to the phosphatidylinositol (PI) cycle and this effect is considered to be the main function of the enzyme.[21] TRPC6 is a calcium-permeable cation channel expressed in the foot processes of podocytes, and is known to be directly activated by DAG through a protein kinase C–independent mechanism.[22] To demonstrate that lack of DGKε affects DAG production in podocytes, we tested the effect of *DGKE* mutations on intracellular DAG concentration, taking advantage of the fact that currents through TRPC6 channels are directly regulated by DAG levels and that, as a consequence, their registration can be used as readout of intracellular DAG abundance.[23] We measured TRPC6 activity by ruptured whole-cell patch-clamp electrophysiological analysis in HEK293T cells cotransfected with TRPC6, M3 muscarinic receptor, and full-length or c.610delA mutant human *DGKE*. No detectable peptide was obtained from the c.127C>T mutant (Figure 3A). TRPC6 currents activated by the M3 receptor agonist carbachol were significantly reduced in cells transfected with wild-type DGKε (Figure 3, B–D), supporting the evidence that the enzyme metabolizes and decreases cellular DAG content. Consistent with the finding that the c.610delA mutation is loss of function, TRPC6 currents in cells expressing the mutant were not different from mock-transfected cells. Because HEK293 cells constitutively express DGKε, we also measured the activity of TRPC6 by electrophysiological analysis after

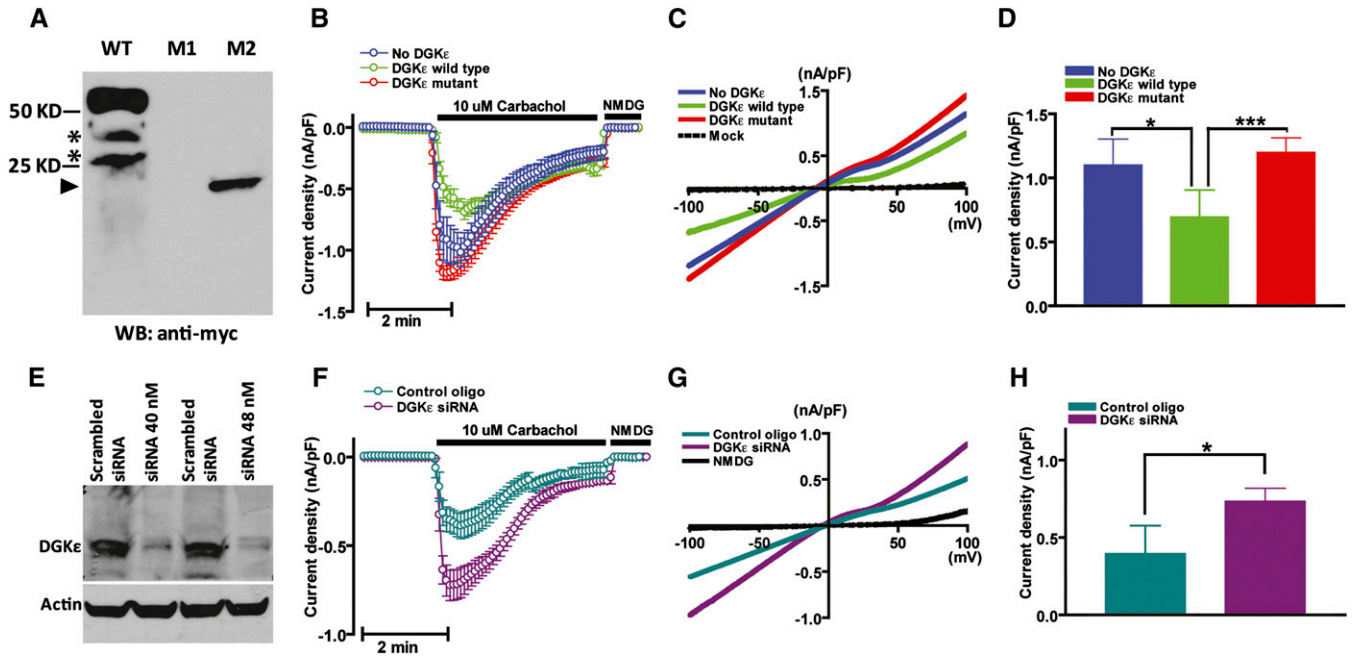

Figure 3. DGKε regulates intracellular DAG levels. (A) Western blot of HEK293T cells transfected with expression vector of myc-tagged wild-type human DGKε (WT) and c.127C>T (M1) and c.610delA (M2) mutants. Nonspecific bands (asterisks) are observed in the WT lane. No peptide was observed overexpressing the c.127C>T mutant. A truncated protein of the expected size (arrowhead at approximately 23 kD) was produced when cells were transfected with the c.610delA mutant. (B) Time course of carbachol (CCh, 10 μM)-induced whole-cell inward TRPC6 current density (nA/pF at −100 mV, mean ± SD, n=20) measured in HEK293T cells transfected with empty expression vector (blue trace), wild-type (green), and c.610delA mutant (red) human DGKε. (C) Current-voltage relationships of currents from B. (D) Mean ± SD of peak inward current density from B. (E) Western blot of HEK293 cells transfected with 40 or 80 nmol of a pool of DGKE-targeting siRNAs or a nontargeting siRNA as control. (F) Time course of carbachol–induced (CCh, 10 μM) whole-cell inward TRPC6 current density measured in HEK293T cells transfected with targeting siRNA (40 nmol, dark green) or nontargeting siRNA as a control (purple). (G) Current-voltage relationships of currents from F. Mean ± SD (n=20) of peak inward current density from F. *P<0.05; ***P<0.001.

suppressing *DGKE* expression with targeting small interfering RNAs (siRNAs) or with nontargeting siRNAs as a control (Figure 3E). In accordance with the previous experiment, TRPC6 currents were increased when DGKε expression was minimal (Figure 3, F–H), indicating that DGKε is required to maintain adequate cellular levels of DAG.

In this study, we have identified mutations in the podocyte expressed gene *DGKE* as the cause of a glomerular microangiopathy with histologic signs of both MPGN and endothelial distress in three unrelated families, by combining whole exome sequencing and homozygosity mapping.[16] Homozygosity mapping is based on the remarkable finding that, for an affected individual born from consanguineous parents, the probability of carrying an autosomal recessive deleterious mutation in a genomic segment that is homozygous by descent is nearly equal to one,[16] which confers a very high statistical power to this technique. We have shown that *DGKE* is expressed in podocytes and controls the intracellular concentration of DAG, a component of the PI cycle that participates in multiple cellular functions and in the lipid-mediated intracellular signaling.[24] Further experiments will be needed to verify if perturbation of this pathway might also affect the signaling between podocytes and endothelial cells, which would explain the vascular lesions observed in our patients. Three of the patients described in this work responded to immunosuppressive therapy (steroids and cyclosporine A or cyclophosphamide) with partial remission, alike a patient affected with diffuse mesangial sclerosis carrying a loss-of-function mutation in the gene *PLCE1*, which encodes for another enzyme of the PI cycle, (Supplemental Figure 4),[25] suggesting that the components of this metabolic and signaling pathway are of particular importance in the physiology of podocytes.

CONCISE METHODS

Genotyping, Homozygosity Mapping, and Sequencing

DNA was extracted with standard procedures from peripheral blood and whole-genome genotyping was performed by 250K NspISNP-chip Affymetrix hybridization array. Exome capture was obtained by using SureSelect Human All Exon 38 Mb reagent kit (Agilent). Captured exons were massively parallel sequenced using a Genome Analyzer IIx (Illumina). Single nucleotide variants and insertion/deletion calls were obtained using CLC Bio Genomic Workbench 4 platform. Sanger exon sequencing was performed in a

worldwide cohort of 142 unrelated patients affected with MPGN.

Whole-Cell Patch-Clamp Electrophysiological Analyses

HEK293T cells were transiently cotransfected with vectors expressing enhanced green fluorescent protein for the identification of the transfected cells, M3 muscarinic receptor, human TRPC6, and wild-type or mutant DGKε. Whole-cell patch-clamp recording was performed using an Axopatch 200B patch-clamp amplifier (Axon Instruments Inc., Foster City, CA) as previously described.[26]

siRNA-Mediated *DGKE* Targeting

A pool of four siRNAs targeting different sequences of *DGKE* mRNA was purchased from Thermo Scientific (SMART pool L-011493-00-0005, anti-human *DGKE* NM_003647) and used according to the manufacturer's indications.

Immunofluorescence Confocal Microscopy

The following antibodies were used: anti-DGKε (sc-98729 and sc-100372) and anti-WT1 (sc-7385), anti-CD31 (MAB1393; Millipore), anti-α-smooth actin (A5228; Sigma), anti-fibrinogen (4440-8004; AbD Serotech), and anti-C3b (Ab11871; Abcam). Specimens were fixed with paraformaldehyde and imbedded in optimal cutting temperature (OCT) compound. Tissue sections were permeabilized in 0.1% Triton X-100 in PBS, incubated in a solution of 0.1% sodium borohydride, blocked in a solution with bovine serum albumin, and incubated overnight at 4°C with primary antibody, followed by incubation with secondary antibody. For the competition assay, the primary antibody was coincubated in blocking solution with a competing peptide at a molar concentration 200 times higher than the antibody, for 1 hour at room temperature. The solution was centrifuged for 5 minutes, and the supernatant was recovered and used on tissue sections. Images were acquired using a Zeiss LSM 510 confocal microscope.

Western Blot Analyses

Equal amounts of protein were mixed with 4× Laemmli sample buffer (Bio-Rad 161-0737) and denatured at 95°C for 10 minutes. Samples were run on 10% polyacrylamide gels, transferred to polyvinylidene difluoride membranes (LC2002), blocked in 5% BSA, and probed with primary and secondary antibodies. Proteins were visualized with Luminol reagent (sc-2048; Santa Cruz).

Site-Directed Mutagenesis

Appropriate mutagenic oligonucleotide primers were designed flanked by unmodified nucleotide sequences and used to amplify full-length *DGKE* cDNA cloned into pCDNA3.1 (Supplemental Table 3). Mutant clones were selected by enzymatic digestion using the QuickChange mutagenesis kit (Agilent).

Quantitative Real-Time PCR

Total RNA was isolated using TRIzol (Invitrogen) and purified with the Qiagen RNeasy Mini Kit according to the manufacturer's protocols. ThermoScript RT-PCR Kit (Invitrogen) was used to obtain first-strand RT. Real-time PCR was performed using iQ SYBR Green Supermix (Bio-Rad). The β actin gene was used as a normalizer.

An exhaustive description of all experiments and methods is available in the Supplemental Material.

ACKNOWLEDGMENTS

We are grateful to the families for their participation to this study. We thank Carlos Arana, Yun Lian, and Georgia Konstantinidou for their technical support and the primary physician of family HU-314, Professor Sukru Sindel, who provided the clinical details of the oldest sibling.

M.A. is supported by grants from the National Institutes of Health (NIH) (1R01DK090326-01A1, P30DK079328-04), a 2010 American Society of Nephrology Norman Siegel Research Award, and a Satellite Healthcare Norman Coplon extramural research award. F.O. was supported by a grant from the Scientific and Technological Research Council of Turkey (108S417). The Nephrogenetics Laboratory at the Hacettepe University Faculty of Medicine, Department of Pediatrics, was established by the Hacettepe University Infrastructure Project (Grant 06A 101 008). F.H. was supported by grants from the NIH (DK1069274, DK1068306, and RC4-DK090947), and is an investigator for the Howard Hughes Medical Institute, a Doris Duke Distinguished Clinical Scientist, and a Frederick G.L. Huetwell Professor. C.H. was supported by grants from the NIH (DK85726) and the University of Texas Southwestern O'Brien Kidney Research Core Center (P30DK79328). M.K.T. was supported by a grant from the NIH (CA095463).

DISCLOSURES

None.

REFERENCES

1. Braun MC, Licht C, Strife CF: Membranoproliferative glomerulonephritis. In: *Pediatric Nephrology*, edited by Avner ED, Harmon WH, Niaudet P, Yoshikawa N, Berlin, Springer, 2009, pp 783–797
2. Sethi S, Fervenza FC: Membranoproliferative glomerulonephritis: Pathogenetic heterogeneity and proposal for a new classification. *Semin Nephrol* 31: 341–348, 2011
3. Bakkaloglu A, Söylemezoglu O, Tinaztepe K, Saatçi U, Söylemezoglu F: Familial membranoproliferative glomerulonephritis. *Nephrol Dial Transplant* 10: 21–24, 1995
4. Berry PL, McEnery PT, McAdams AJ, West CD: Membranoproliferative glomerulonephritis in two sibships. *Clin Nephrol* 16: 101–106, 1981
5. Bogdanović RM, Dimitrijević JZ, Nikolić VN, Ognjanović MV, Rodić BD, Slavković BV: Membranoproliferative glomerulonephritis in two siblings: Report and literature review. *Pediatr Nephrol* 14: 400–405, 2000
6. Walker PD, Ferrario F, Joh K, Bonsib SM: Dense deposit disease is not a membranoproliferative glomerulonephritis. *Mod Pathol* 20: 605–616, 2007
7. Buddles MR, Donne RL, Richards A, Goodship J, Goodship TH: Complement factor H gene mutation associated with autosomal recessive atypical hemolytic uremic syndrome. *Am J Hum Genet* 66: 1721–1722, 2000
8. Veyradier A, Obert B, Haddad E, Cloarec S, Nivet H, Foulard M, Lesure F, Delattre P, Lakhdari M, Meyer D, Girma JP, Loirat C: Severe deficiency of the specific von Willebrand factor-cleaving protease (ADAMTS 13) activity in a subgroup of children with atypical hemolytic uremic syndrome. *J Pediatr* 142: 310–317, 2003
9. Noris M, Brioschi S, Caprioli J, Todeschini M, Bresin E, Porrati F, Gamba S, Remuzzi G; International Registry of Recurrent and Familial HUS/TTP: Familial haemolytic uraemic syndrome and an MCP mutation. *Lancet* 362: 1542–1547, 2003
10. Brackman D, Sartz L, Leh S, Kristoffersson AC, Bjerre A, Tati R, Frémeaux-Bacchi V, Karpman D: Thrombotic microangiopathy

mimicking membranoproliferative glomerulonephritis. *Nephrol Dial Transplant* 26: 3399–3403, 2011
11. Chen LT, Gilman AG, Kozasa T: A candidate target for G protein action in brain. *J Biol Chem* 274: 26931–26938, 1999
12. Kumar P, Henikoff S, Ng PC: Predicting the effects of coding non-synonymous variants on protein function using the SIFT algorithm. *Nat Protoc* 4: 1073–1081, 2009
13. 1000 Genomes Project Consortium: A map of human genome variation from population-scale sequencing. *Nature* 467: 1061–1073, 2010
14. Tennessen JA, Bigham AW, O'Connor TD, Fu W, Kenny EE, Gravel S, McGee S, Do R, Liu X, Jun G, Kang HM, Jordan D, Leal SM, Gabriel S, Rieder MJ, Abecasis G, Altshuler D, Nickerson DA, Boerwinkle E, Sunyaev S, Bustamante CD, Bamshad MJ, Akey JM; Broad GOSeattle GONHLBI Exome Sequencing Project: Evolution and functional impact of rare coding variation from deep sequencing of human exomes. *Science* 337: 64–69, 2012
15. Kohyama-Koganeya A, Watanabe M, Hotta Y: Molecular cloning of a diacylglycerol kinase isozyme predominantly expressed in rat retina. *FEBS Lett* 409: 258–264, 1997
16. Lander ES, Botstein D: Homozygosity mapping: A way to map human recessive traits with the DNA of inbred children. *Science* 236: 1567–1570, 1987
17. Bamshad MJ, Ng SB, Bigham AW, Tabor HK, Emond MJ, Nickerson DA, Shendure J: Exome sequencing as a tool for Mendelian disease gene discovery. *Nat Rev Genet* 12: 745–755, 2011
18. Rodriguez de Turco EB, Tang W, Topham MK, Sakane F, Marcheselli VL, Chen C, Taketomi A, Prescott SM, Bazan NG: Diacylglycerol kinase epsilon regulates seizure susceptibility and long-term potentiation through arachidonoyl- inositol lipid signaling. *Proc Natl Acad Sci U S A* 98: 4740–4745, 2001
19. Sanden SK, Wiggins JE, Goyal M, Riggs LK, Wiggins RC: Evaluation of a thick and thin section method for estimation of podocyte number, glomerular volume, and glomerular volume per podocyte in rat kidney with Wilms' tumor-1 protein used as a podocyte nuclear marker. *J Am Soc Nephrol* 14: 2484–2493, 2003
20. Epand RM, Topham MK: Measurement of mammalian diacylglycerol kinase activity in vitro and in cells. *Methods Enzymol* 434: 293–304, 2007
21. Tang W, Bunting M, Zimmerman GA, McIntyre TM, Prescott SM: Molecular cloning of a novel human diacylglycerol kinase highly selective for arachidonate-containing substrates. *J Biol Chem* 271: 10237–10241, 1996
22. Hofmann T, Obukhov AG, Schaefer M, Harteneck C, Gudermann T, Schultz G: Direct activation of human TRPC6 and TRPC3 channels by diacylglycerol. *Nature* 397: 259–263, 1999
23. Reiser J, Polu KR, Möller CC, Kenlan P, Altintas MM, Wei C, Faul C, Herbert S, Villegas I, Avila-Casado C, McGee M, Sugimoto H, Brown D, Kalluri R, Mundel P, Smith PL, Clapham DE, Pollak MR: TRPC6 is a glomerular slit diaphragm-associated channel required for normal renal function. *Nat Genet* 37: 739–744, 2005
24. Mérida I, Avila-Flores A, Merino E: Diacylglycerol kinases: At the hub of cell signalling. *Biochem J* 409: 1–18, 2008
25. Hinkes B, Wiggins RC, Gbadegesin R, Vlangos CN, Seelow D, Nürnberg G, Garg P, Verma R, Chaib H, Hoskins BE, Ashraf S, Becker C, Hennies HC, Goyal M, Wharram BL, Schachter AD, Mudumana S, Drummond I, Kerjaschki D, Waldherr R, Dietrich A, Ozaltin F, Bakkaloglu A, Cleper R, Basel-Vanagaite L, Pohl M, Griebel M, Tsygin AN, Soylu A, Müller D, Sorli CS, Bunney TD, Katan M, Liu J, Attanasio M, O'toole JF, Hasselbacher K, Mucha B, Otto EA, Airik R, Kispert A, Kelley GG, Smrcka AV, Gudermann T, Holzman LB, Nürnberg P, Hildebrandt F: Positional cloning uncovers mutations in PLCE1 responsible for a nephrotic syndrome variant that may be reversible. *Nat Genet* 38: 1397–1405, 2006
26. Cha SK, Ortega B, Kurosu H, Rosenblatt KP, Kuro-O M, Huang CL: Removal of sialic acid involving Klotho causes cell-surface retention of TRPV5 channel via binding to galectin-1. *Proc Natl Acad Sci U S A* 105: 9805–9810, 2008

See related editorial, "Lipid Kinase Mutations in Heritable Glomerular Microangiopathy," on pages 329–330.

This article contains supplemental material online at http://jasn.asnjournals.org/lookup/suppl/doi:10.1681/ASN.2012090903/-/DCSupplemental.